

Computed reference computed torque control of the end-effector of a flexible 2D translation robot

Citation for published version (APA):

Willems, F. P. T. (1994). *Computed reference computed torque control of the end-effector of a flexible 2D translation robot*. (DCT rapporten; Vol. 1994.160). Technische Universiteit Eindhoven.

Document status and date:

Published: 01/01/1994

Document Version:

Publisher's PDF, also known as Version of Record (includes final page, issue and volume numbers)

Please check the document version of this publication:

- A submitted manuscript is the version of the article upon submission and before peer-review. There can be important differences between the submitted version and the official published version of record. People interested in the research are advised to contact the author for the final version of the publication, or visit the DOI to the publisher's website.
- The final author version and the galley proof are versions of the publication after peer review.
- The final published version features the final layout of the paper including the volume, issue and page numbers.

[Link to publication](#)

General rights

Copyright and moral rights for the publications made accessible in the public portal are retained by the authors and/or other copyright owners and it is a condition of accessing publications that users recognise and abide by the legal requirements associated with these rights.

- Users may download and print one copy of any publication from the public portal for the purpose of private study or research.
- You may not further distribute the material or use it for any profit-making activity or commercial gain
- You may freely distribute the URL identifying the publication in the public portal.

If the publication is distributed under the terms of Article 25fa of the Dutch Copyright Act, indicated by the "Taverne" license above, please follow below link for the End User Agreement:

www.tue.nl/taverne

Take down policy

If you believe that this document breaches copyright please contact us at:

openaccess@tue.nl

providing details and we will investigate your claim.

† †

**COMPUTED REFERENCE COMPUTED TORQUE
CONTROL OF THE END-EFFECTOR OF A
FLEXIBLE 2D TRANSLATION ROBOT**

Frank Willems

WFW report nr. 94.160

† †

Coach : dr.ir. M.J.G. van de Molengraft

Chair : prof.dr.ir. J.J. Kok

Eindhoven University of Technology (TUE)

Department of Mechanical Engineering

Division of Mechanical Engineering Fundamentals (WFW)

Abstract

Today's industry shows an increasing demand for flexible manipulators. As the control of these systems by conventional control concepts lead to inaccurate movements, there is a need for control concepts which deal with the flexibility of joints and links. During a recent Ph.D. study, a new control concept has been developed for the control of flexible manipulators: *Adaptive Computed Reference Computed Torque Control (ACRCTC)*. This strategy showed good results for the joint-level control of a 2D flexible translation robot. However, in practice, one is interested in the movements of the end-effector. Therefore, this study is concerned with the implementation of the *direct CRCTC* strategy on the XY-table.

This report is partly devoted to some practical facets of the implementation of the CRCTC strategy because little is known about it. The possibilities of the implemented control strategy are investigated for a set-point tracking and a trajectory tracking control problem. The simulations show promising results for both control problems; the end-effector tracks the desired trajectory fast and reasonably accurate in spite of the flexibility of the spindle. It is expected that the quality of the results will substantially decrease for experiments.

Contents

1	Introduction	2
2	CRCTC of the XY-table	3
2.1	Introduction	3
2.2	The experimental set-up	3
2.3	The model of the XY-table	4
2.4	The CRCTC scheme for the XY-table	5
3	Implementation of the CRCTC strategy	7
3.1	Introduction	7
3.2	Implementation of the CRCTC strategy	7
4	Simulations	9
4.1	Introduction	9
4.2	Set-point tracking	9
4.2.1	The control problem	9
4.2.2	Discussion of the results	9
4.3	Trajectory tracking	13
4.3.1	The control problem	13
4.3.2	Discussion of the results	14
5	Conclusions and recommendations	17
5.1	Conclusions	17
5.2	Recommendations	17
	References	18
A	The model of the XY-table	19
A.1	The flexible model of the XY-table	19
A.2	The coordinate transformation	20
B	Results of the set-point tracking problem	21
B.1	The model parameters	21
B.2	The results of simulations	22
C	Results of the trajectory tracking problem	23
C.1	The results of the simulations	23

Chapter 1

Introduction

Manipulators are used to perform tasks like arc welding, paint spraying and parts assembling. These tasks are defined in terms of motion of the end-effector. Most of today's manipulators are designed stiff in order to avoid significant deformations and vibrations and to obtain the desired positioning and tracking accuracy. As a consequence, these manipulators are quite heavy and unwieldy. Increasing demands on accelerations, on the precision and on the energy consumption require lightweight manipulators. However, lightweight manipulators introduce elastic deformations and vibrations during rapid movements and can cause instability if the controller is designed under the assumption of perfect rigidity. In this case, a more complex control concept is required which accounts for flexibility.

Recently, a control scheme is introduced that handles with the above mentioned problem: *Adaptive Computed Reference Computed Torque Control (ACRCTC)*. This Computed Torque Control scheme is based on a model that takes flexibility of joints and/or links into account. Instead of suppressing the vibrations, this strategy applies such inputs that the elastic deformations remain bounded. Former research dealt with the implementation of this strategy on a 2D flexible translation robot, the XY-table. Simulations and experiments showed promising results for joint-level control; the control objective has been realized indirectly by controlling the joint-coordinates. In practice, one is interested in the movements of the end-effector. This is comparable with writing a letter: you control the movements of your hand with the position information which you obtain from your eyes. Therefore, this study is focussed on *direct control* of the end-effector: the desired trajectory is formulated in terms of the position of the end-effector and feedback control is based on measurements of this position by a camera.

The overall objective of this study is the implementation of the direct CRCTC strategy for the XY-table. First of all, a model of the experimental set-up is needed to restrict the CRCTC law for the XY-table. The applied model and the CRCTC strategy are discussed in Chapter 2. Chapter 3 deals with the implementation of the CRCTC law and illustrates the used software packages. The results of the simulations are discussed in Chapter 4. Finally, Chapter 5 shows the conclusions and put forward some suggestions for future work.

Chapter 2

CRCTC of the XY-table

2.1 Introduction

In this study the XY-table is used to test the direct CRCTC concept. The experimental set-up is described in section 2.2. As the CRCTC scheme is a model based approach, the applied model of the XY-table is given in section 2.3. The CRCTC strategy and the derivation of the CRCTC scheme for the XY-table are briefly discussed in section 2.4.

2.2 The experimental set-up

The XY-table, see figure 2.1, is a translation-translation manipulator which consists of two slide-ways in X-direction and a transverse slideway with the end-effector.

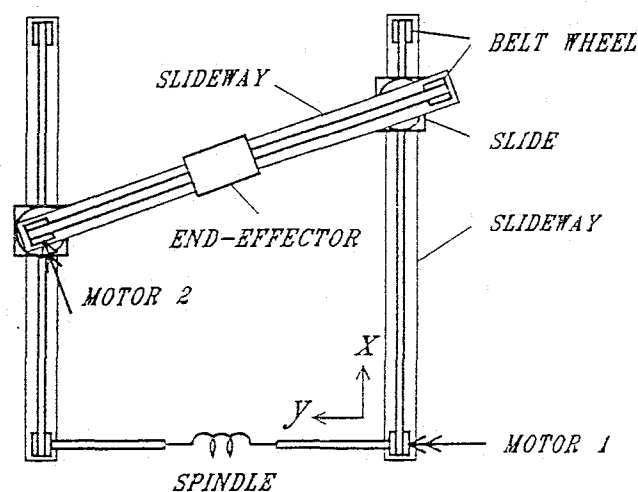


Figure 2.1: The experimental set-up

The motors generate the torques u_1 and u_2 for the X- and Y-translation respectively. The belt wheels of the two slides in X-direction are connected to a spindle that is driven via a transmission by motor 1. Along the transverse slideway, the end-effector is belt driven by motor 2.

The stiffness of the spindle can easily be changed in a broad range. If the spindle is flexible, its elastic deformation introduces an extra degree of freedom. Consequently, the movements of

the end-effector along the Y-slideway will no longer be equal to moving in Y-direction.

2.3 The model of the XY-table

The applied model of the XY-table (Heeren [5]) is depicted in figure 2.2:

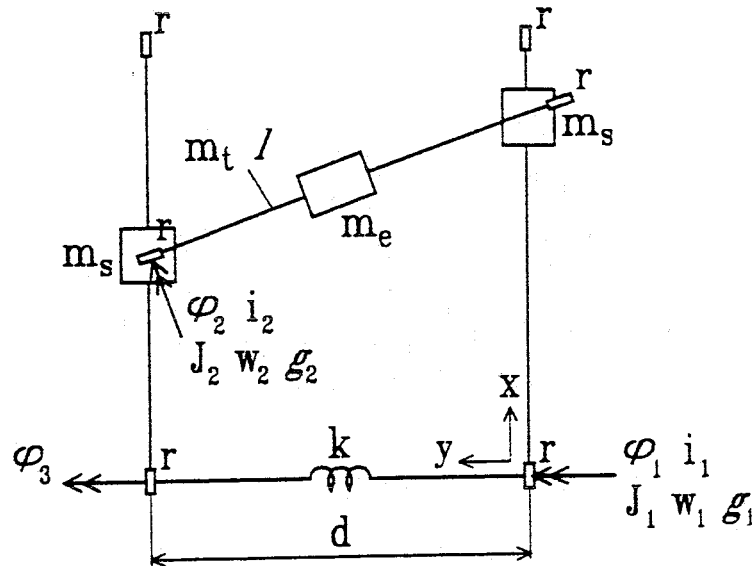


Figure 2.2: Model of the XY-table

With the following meaning of the symbols:

- φ_1 : rotation of motor 1 [rad]
- φ_2 : rotation of motor 2 [rad]
- φ_3 : rotation of the non-driven end of the spindle [rad]
- i_j : current applied to motor j ; $j=1,2$ [A]
- J_j : rotor inertia of motor j [kgm^2]
- w_j : Coulomb friction torques at motor j [Nm]
- m_e : mass of the end-effector [kg]
- m_s : mass of the slide [kg]
- m_t : mass of the transverse slideway [kg]
- k : torsion stiffness of the spindle [Nm/rad]
- d : distance between the parallel slideways [m]
- l : length of the transverse slideway [m]
- r : radius of the belt wheels [m]

As this study is concerned with flexible manipulators, only the flexible model of the XY-table is discussed here. Except the spindle, the drives and transmissions in this model are assumed to be rigid. This also applies to the slideways of the manipulator. Further, viscous friction is supposed to be neglectable and the friction between belt wheels and belts is assumed to be small with regard to the Coulomb friction in the motors.

The dynamic model of the XY-table is of the following form:

$$M(\underline{\varphi})\ddot{\underline{\varphi}} + C(\underline{\varphi}, \dot{\underline{\varphi}})\dot{\underline{\varphi}} + K\underline{\varphi} + \underline{w}sign(\dot{\underline{\varphi}}) = H\underline{u} \quad (2.1)$$

where $\underline{\varphi}$ is the column of the generalized coordinates $\underline{\varphi} = [\varphi_1 \ \varphi_2 \ \varphi_3]^T$ and \underline{u} is the column of input torques. The term $C(\underline{\varphi}, \dot{\underline{\varphi}})\dot{\underline{\varphi}}$ accounts for Coriolis and centrifugal effects, $K\underline{\varphi}$ represents all internal torques due to linear, elastic deformations and $\underline{w}sign(\dot{\underline{\varphi}})$ describes the torques due to Coulomb friction in the system. The matrix H is the so called distribution matrix and the torques u_j are assumed to be proportional to the motor currents i_j , i.e. $u_j = g_j \cdot i_j$. A detailed description of the dynamic model of the XY-table can be found in Appendix A.

For direct control of the end-effector, the coordinates x and y have to be controlled instead of φ_1 and φ_2 so that a new set of generalized coordinates can be used. In that case, a coordinate transformation has to be performed on the dynamic model (2.1). This transformation also contains a substitution of the flexible coordinate φ_3 by x_3 , i.e. the position $[m]$ of the slide along the slave X-slideway, because of the desire for a model with uniform dimensions. This facilitates the physical interpretation of the results. The new set of generalized coordinates $\underline{y} = [x \ y \ x_3]^T$ is related to $\underline{\varphi}$ according to

$$\underline{\varphi} = \Phi \underline{y}. \quad (2.2)$$

Here, Φ is continuous and differentiable with derivative Ψ :

$$\Psi_{ij} = \frac{\delta \Phi_i}{\delta y_j} \quad (2.3)$$

After coordinate transformation the new model is given by

$$M^*\ddot{\underline{y}} + C^*\dot{\underline{y}} + K^*\underline{y} + \underline{w}sign(\dot{\underline{y}}) = H\underline{u} \quad (2.4)$$

where $M^* = M\Psi$, $C^* = M\dot{\Psi} + C\Psi$ and $K^* = K\Phi$. The superscript $*$ is omitted in the rest of this report because it is clear when the transformed system is used.

For the sake of completeness, it is noted that the feedback information of the coordinates x and y is obtained from camera measurements of the end-effector position while the flexible coordinate is determined from incremental optical encoder measurements of the rotation at the non-driven end of the flexible spindle. However, this report only contains the results of simulations.

For a detailed description of the coordinate transformation, see Appendix A.

2.4 The CRCTC scheme for the XY-table

The CRCTC strategy (Lammerts [7]) is applied in order to cope with the flexibility of the XY-table. This control strategy is illustrated from figure 2.3. The CRCTC scheme is based on the *Computed Torque Control (CTC)* approach which compensates for nonlinearities. The main problem in controlling a flexible manipulator is that the number of actuators is smaller than the number of degrees of freedom. Usually, the applied control schemes attempt to suppress the elastic deformations in order to obtain asymptotic trajectory tracking of the end-effector. However, the CRCTC scheme attempts to realize this objective by restricting the vibrations in the drives and links to an acceptable level. Therefore, a *reference trajectory* is computed for the flexible coordinates.

The reference trajectory \underline{y}_r is related to the desired trajectory \underline{y}_d in the following manner:

$$\dot{\underline{y}}_r = \dot{\underline{y}}_d + \Lambda \underline{e} \quad \underline{e} = \underline{y}_d - \underline{y} \quad (2.5)$$

where $\Lambda + \Lambda^T$ is a positive definite matrix.

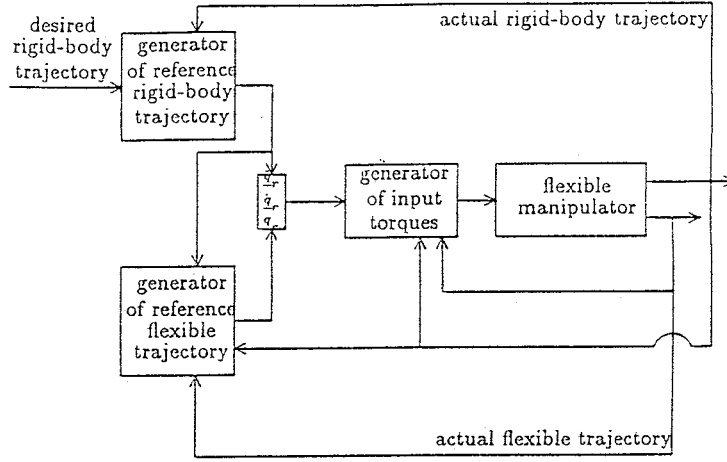


Figure 2.3: Global block scheme of CRCTC

The determination of the reference trajectory of the flexible coordinates $\underline{\rho}_r$ is based on the property of Eq.(2.4) that it can be split in a set of equations that contain the input and a set of nonlinear differential equations that do not contain the input.

$$H\underline{u} = M\underline{\ddot{y}}_r + C\underline{\dot{y}}_r + K\underline{y}_r + \underline{w} \text{sign}(\underline{\dot{y}}) + K_r \underline{\dot{e}}_r ; \quad \underline{\dot{e}}_r = \underline{\dot{y}}_r - \underline{\dot{y}} \quad (2.6)$$

$$M_\rho \underline{\ddot{\rho}}_r + M_\theta \underline{\ddot{\theta}}_r + C_\rho \underline{\dot{\rho}}_r + C_\theta \underline{\dot{\theta}}_r + K_\rho \underline{\rho}_r + K_\theta \underline{\theta}_r + \underline{w}_\rho \text{sign}(\underline{\dot{\rho}}) + K_r \underline{\dot{e}}_r = \underline{0} \quad (2.7)$$

For better survey, the matrices in Eq.(2.7) are partitioned in terms of the rigid coordinates $\underline{\theta}_r$ and the flexible coordinates $\underline{\rho}_r$. The input commands lead to the following error equation for the closed loop system:

$$M \underline{\ddot{e}}_r + C \underline{\dot{e}}_r + K_r \underline{\dot{e}}_r + K \underline{e}_r = \underline{0} \quad (2.8)$$

With the use of Lyapunov's second method, it can be proven that asymptotic tracking of the desired end-effector trajectory is achieved if a bounded solution $\underline{\rho}_r = \underline{\rho}_r(t)$ can be determined from Eq.(2.7).

For the presence of parametric uncertainty and unmodeled dynamics, an adaptive scheme can be added to the CRCTC scheme in order to realize better trajectory tracking.

The implementation of this strategy on the XY-table is elaborated in the next chapter.

Chapter 3

Implementation of the CRCTC strategy

3.1 Introduction

A considerable part of this research is devoted to the realization of the implementation of the CRCTC strategy on the XY-table. This chapter deals with some practical facets of the implementation in order to give better insight in the used methods, especially the applied software packages. However, this should not be seen as a detailed manual.

3.2 Implementation of the CRCTC strategy

The software that is used for the implementation is illustrated from figure 3.1.

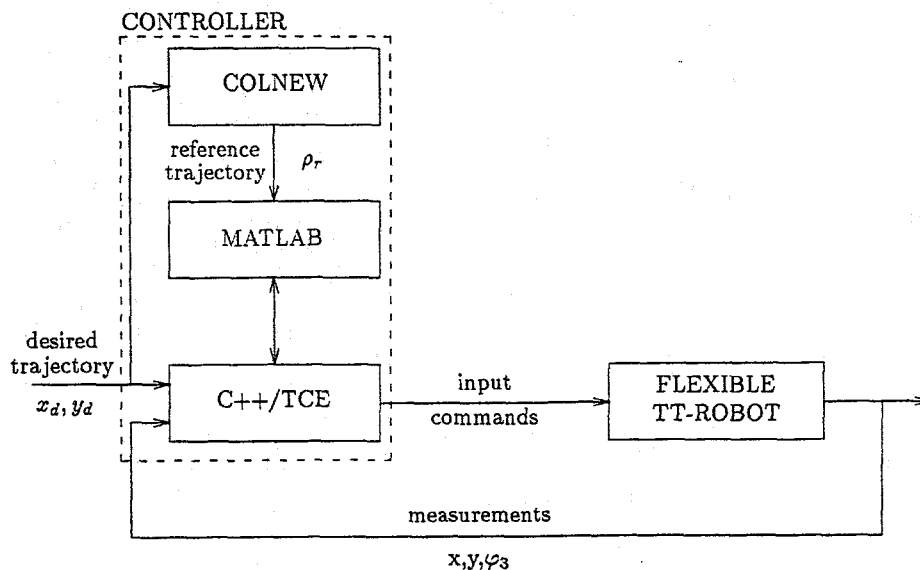


Figure 3.1: A block scheme of the experimental set-up with software

The main problem of the CRCTC strategy is the determination of a bounded solution $\rho_r = \rho_r(t)$. Unfortunately, this is not always possible since Eq.(2.7) may be unstable. In this study, the FORTRAN-package COLNEW is used to solve the nonlinear second order differential equation.

COLNEW is based on the collocation technique and solves boundary value problems for ordinary differential equations (Ascher et al. [1]). This method requires all quantities to be available for each time in the interval $[t, t_e]$. As this is certainly not the case in practice, this problem is solved under the assumption that the desired trajectory is already achieved; the reference quantities and the actual generalized velocities are replaced by the desired quantities and the term $K_r \dot{e}_r$ is neglected. Although this solution is only an approximate solution of the differential equation, former research (Lammerts [7]) showed good results for this method. It is noted that either the actual generalized coordinates nor the actual generalized velocities occur in the modified differential equation. Hence, the computation of the solution can be done *off-line*.

The control commands \underline{u} can be computed if the reference trajectory $\underline{\rho}_r$ is available. The control law will be called the *modified* CRCTC law as it makes use of the off-line computed *desired* trajectory of the flexible coordinate. The determination of \underline{u} also requires the second derivative of $\underline{\rho}_d$ to be available.¹

Further, the control strategy needs information about the actual generalized velocities \dot{x} , \dot{y} and \dot{x}_3 . Possible ways to yield this quantities are the application of a numerical weak differential scheme or a Kalman filter. For the sake of simplicity, the Euler differential scheme is used here:

$$\left[\frac{\delta y}{\delta t} \right]_{i+1} = \frac{y(i+1) - y(i)}{T} \quad (3.1)$$

where T is the sample time, and $\underline{y}(i)$ are the available measurements on the i^{th} sample moment.

For experiments, the input commands have to be C++ coded by the user and can be applied to the XY-table with the use of the available TCE-modules (Banens [2]). These modules are coded in C++ and implement basic tools to do experiments. At the same time, this standard experiment interface encourages simple plug-in of a simulator. Both a 3 D.O.F. flexible model as a 2 D.O.F. rigid model of the XY-table are available. The simulator contains a dynamic model of the XY-table in the generalized coordinates x_1 , x_2 (and x_3 for the flexible system) i.e. the position of the slides and end-effector along the slideways. As a consequence, the estimated model parameters in Lammerts [7] has to be transformed into the desired quantities, see appendix B. This transformation can be applied with use of methods as described in Koster [6]. For further details about the simulator, see Banens [3].

As it is hardly possible to translate COLNEW in C code, MATLAB has to be used as an 'intermedium' to load the computed trajectory $\underline{\rho}_d$ in the C++ program that contains the CRCTC law. Further, MATLAB is used to analyse the results of the simulations or the experiments.

¹ $\ddot{\underline{\rho}}_d$ can be solved from Eq.(2.7) with use of the determined $\dot{\underline{\rho}}_d$ and $\underline{\rho}_d$. However, this solution yields abnormal high acceleration gains which give rise to serious control problems. Therefore, $\ddot{\underline{\rho}}_d$ is computed in MATLAB with use of the function DIFF.

Chapter 4

Simulations

4.1 Introduction

The performance of the implemented control strategy is investigated for two control problems: set-point tracking and trajectory tracking. The results of these simulations are discussed in this chapter and are compared with a Computed Torque Control strategy.

4.2 Set-point tracking

4.2.1 The control problem

The first test case for the CRCTC strategy is the set-point tracking problem. The control objective is position control of the end-effector i.e. stabilization of the manipulator around a desired operating point. This is of interest for e.g. pick-and-place and assembly tasks of manipulators.

The set-point tracking problem turns Eq.(2.7) into a constant linear second order differential equation:

$$M_\rho \ddot{\rho}_d + K_\rho \rho_d = K_\theta \underline{\theta}_d - w_3 \text{sign}(\dot{\rho}_d) \quad (4.1)$$

where $\underline{\theta}_d = [x_d \ y_d]^T$ and $\rho_d = x_{3d}$. In order to determine a solution for the flexible coordinate x_{3d} , this problem is formulated as a *two point boundary value problem* in COLNEW: the solution has to meet the boundary conditions $\rho_d(0) = \rho_d(t_e)$ and $\dot{\rho}_d(0) = \dot{\rho}_d(t_e)$ where t_e stands for the end time of the simulation. COLNEW yields the constant solution $\rho_d(t) = x_d$ for this problem. This is plausible if one considers that the term $K_\theta \underline{\theta}_d$ can be written as $K_\rho x_d = C$; the only possible periodical solution is this constant solution.

The end-effector starts for all these simulations in $O(0,0)$ with velocity $\underline{\dot{y}} = \underline{0}$ and has to be stabilized in the operating point $x_d = 0.10[m]$ and $y_d = 0.15[m]$. The simulations are done with a sampling frequency of $200[Hz]$. For the results of the set-point tracking problem, see Appendix B.

4.2.2 Discussion of the results

First of all, these simulations are done in order to find suitable values for the control gains Λ and K_r . Both the recommended values in Lammerts [7] and the relation $x_i = r\varphi_i$ ($r = .01[m]$) are used as starting point to estimate the magnitudes of the gains of the direct control problem.

$$K_r(\dot{\varphi}_{ir} - \dot{\varphi}_i) = 100K_r(\dot{x}_{ir} - \dot{x}_i) \quad (4.2)$$

From Eq.(4.2), it can be concluded that the recommended gains of K_r has to be roughly multiplied with a factor 100 and Λ has to remain unchanged. As asymmetry can occur in the tracking errors, an extra integral-like control term $K_i \underline{e}_r$ is added to Eq.(2.6). All the simulations are started with

the determination of K_r and Λ while $K_i=0$. If acceptable results are achieved, K_i is used to stabilize the drift of e_r . For the sake of simplicity, these matrices are chosen to be diagonal.

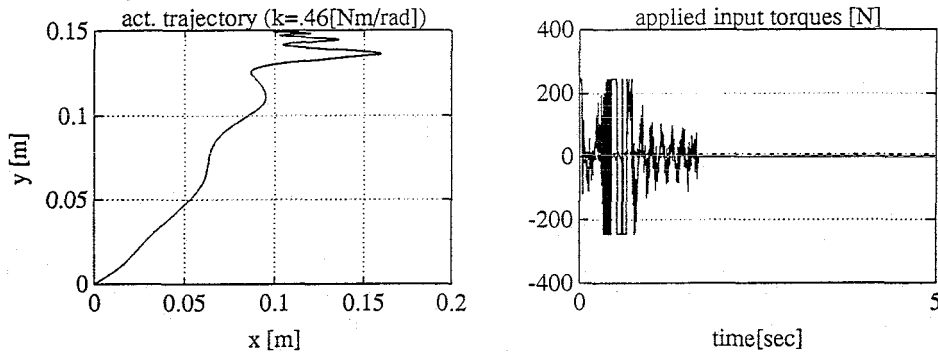


Figure 4.1: The described trajectory of the end-effector and the applied input torques u_1 (-) and u_2 (-.) for the CRCTC strategy ($k=.46$ [Nm/rad])

As far as the choice of the control gains goes, it can be noted that the bigger the control gains of Λ (with constant K_r) the faster the desired position is achieved. As expected, the coordinates x and x_3 have to be weighted more heavily than the Y-coordinate because the influence of the flexible spindle is felt in X-direction. The control matrix K_r adjusts the damping of the error system. Suitable values for the XY-table with the most flexible spindle are $K_r=\text{diag}[30 \ 10 \ 0]$, $\Lambda=\text{diag}[6 \ 4 \ 6]$ and $K_i=\text{diag} [.5 \ .4 \ 0]$. The third element of K_r and K_i is zero because these terms are neglected in the differential equation and do not exist in the control law.

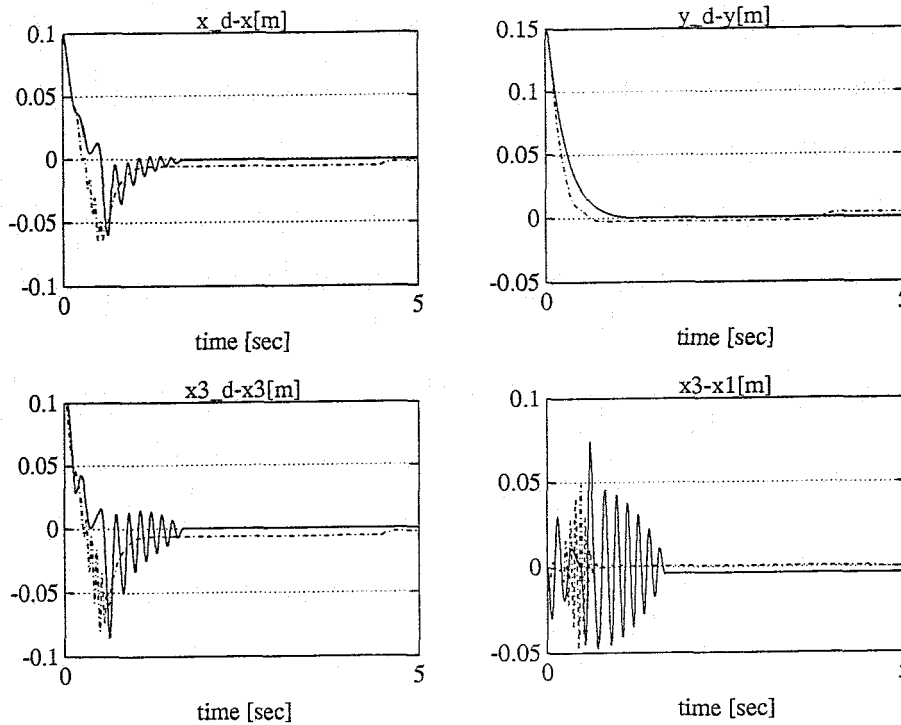


Figure 4.2: The tracking errors and elastic deformation for the CRCTC strategy for $k=.46$ [Nm/rad] (-) and $k=2.55$ [Nm/rad] (-.)

It is noted that it is tried to find a compromise between the fastness of the controlled system, the positioning accuracy and the required input commands in this study. Figure B.1 shows the results of a 'soft' controlled system ($K_r = \text{diag}[30 \ 10 \ 0]$, $\Lambda = \text{diag}[2 \ 1 \ 2]$ and $K_i = \text{diag}[-.5 \ .3 \ 0]$). However, the starting point of the CRCTC strategy is the realization of fast flexible manipulators which can be moved with high precision. These exacting demands can lead to great efforts of the actuators. As long as no 'bang-bang' controller is realized, a short term chattering effect is accepted. The torques of motor 1 are clipped to 246 [N] and motor 2 to 41 [N]. The results that are presented in this report give an impression of the maximal realizable performance when the existing actuators are used.

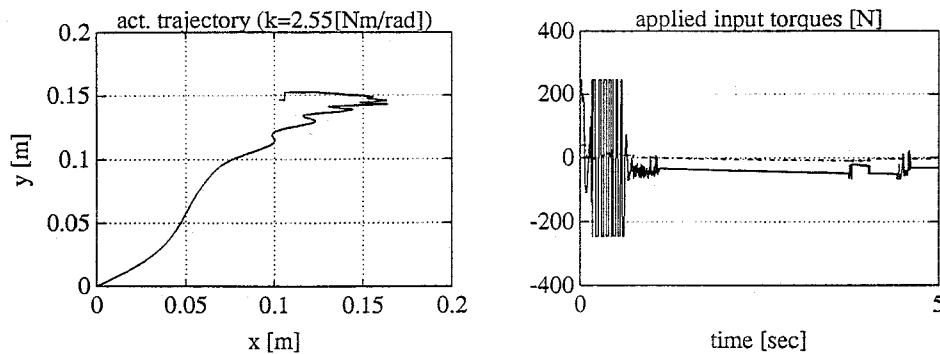


Figure 4.3: The described trajectory of the end-effector and the applied input torques u_1 (-) and u_2 (-) for the CRCTC strategy ($k=2.55$ [Nm/rad])

The results for the most flexible spindle, $k=.46$ [Nm/rad], are depicted in figure 4.1 and 4.2. The desired operational point is achieved with an accuracy of 2[mm] in approximately 1[s]. The coordinates x and x_3 show a vibration with a frequency that is roughly equal to the undamped natural frequency of the spindle, $f_0=7$ [Hz]. It is concluded from this vibrations and the elastic deformation $x_3 - x_1$ that the CRCTC law incorporates explicitly the flexibility of the spindle. The input u_1 shows a 'chattering' effect at the begin of the simulation which leads to actuator saturation at some moments. The controller yields these torques in order to realize the vibration of the spindle. From .7[s], the controller generates smaller input commands because the vibration has to be damped and the end-effector has to be positioned in the desired operation point.

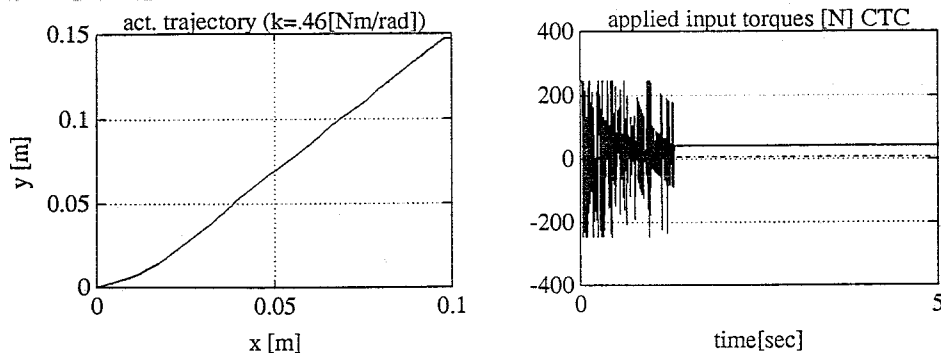


Figure 4.4: The described trajectory of the end-effector and the applied input torques u_1 (-) and u_2 (-) for the CTC strategy ($k=.46$ [Nm/rad])

Further, the influence of the flexibility is investigated: simulations are done with $k=2.55$ [Nm/rad], see figure 4.2 and 4.3 ($K_r=\text{diag}[8 \ 2 \ 0]$, $\Lambda=\text{diag}[8 \ 6 \ 8]$ and $K_i=\text{diag} [.5 \ .4 \ 0]$). These results are comparable with the most flexible system but this control problem requires relatively smoother input torques. This is expected as the elastic deformation will be reduced on behalf of the increased stiffness of the spindle. Consequently, the actuators have to supply smaller input torques in order to realize good results. The coordinates x and x_3 show a vibration with the undamped natural frequency of the new spindle, $f_0=16$ [Hz].

The results of the CRCTC strategy are compared with a version of the classical CTC method for flexible manipulators:

$$H\underline{u} = M(\underline{\ddot{y}}_d + L_d\underline{\dot{e}} + L_p\underline{e}) + C\underline{\dot{y}} + K\underline{y} + \underline{w} \text{sign}(\underline{\dot{y}}) \quad (4.3)$$

where $\underline{e} = \underline{y}_d - \underline{y}$. This control law results in a quite simple error equation:

$$\underline{\ddot{e}} + L_d\underline{\dot{e}} + L_p\underline{e} = \underline{0} \quad (4.4)$$

If the control matrices are constant with a positive definite symmetric part, this error equation has a unique, globally, asymptotically stable equilibrium $\underline{e} = \underline{0}$. Here, $L_p = \omega_0^2 I$ and $L_d = 2\beta_0\omega_0 I$ so that the error equations decouple and the choice of the remaining control parameters ω_0 and β_0 can be based on well known concepts of linear, constant second-order systems.

The CTC method for flexible manipulators determines a desired trajectory of the flexible coordinate in a comparable way with the CRCTC strategy. Lammerts describes this so called *Computed Desired Computed Torque Control* strategy in [7]. However, the flexible coordinate x_{3d} is approximated by $x_{3d}(t) = x_d(t)$ in this study as this comparison is only intended to get a global impression of the value of the results of the CRCTC strategy.

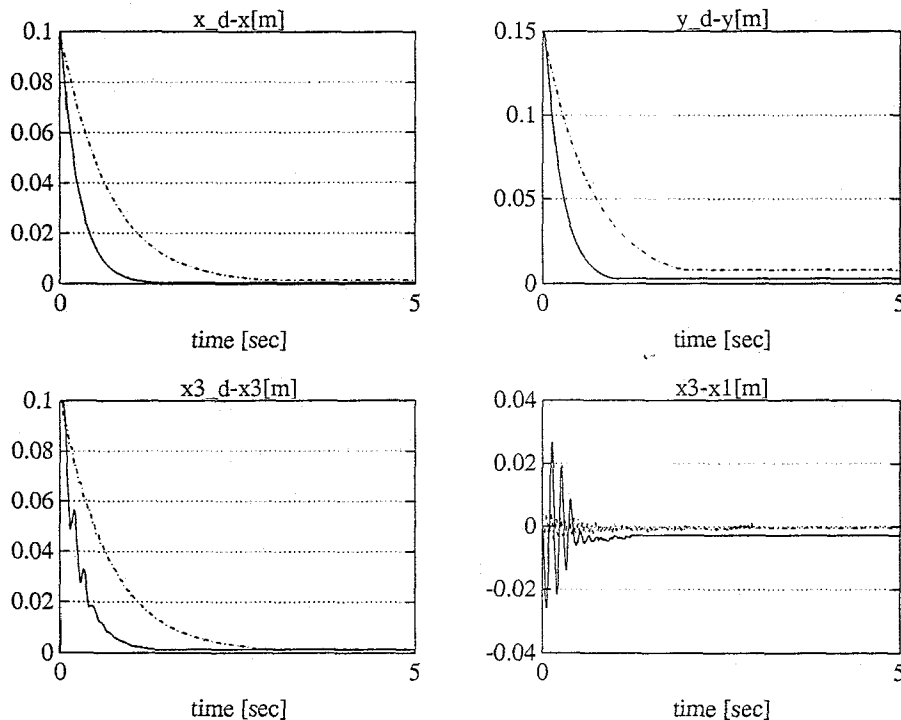


Figure 4.5: The tracking errors and elastic deformations for the CTC strategy for $k=.46$ [Nm/rad] (-) and $k=2.55$ [Nm/rad] (-.)

The results of the CTC controller for the most flexible system are depicted in figure 4.4 and 4.5. The operational point is achieved as fast and accurate as with the CRCTC method. It can be made clear that the elastic deformations are relatively small because the desired flexible coordinate x_{3d} is equal to x_d so that the applied method does not explicitly account for the flexibility in the system. The input torque u_1 of the CTC method also shows the chattering effect. This is a consequence of the required high control gains, $\omega_0=25[\text{rad/s}]$ and $\beta_0=3$, in order to realize the best compromise.

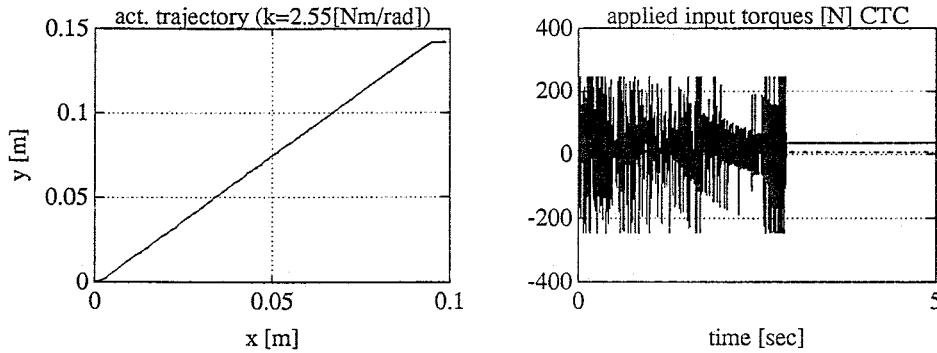


Figure 4.6: The described trajectory of the end-effector and the applied input torques u_1 (-) and u_2 (-.) for the CTC strategy ($k=2.55$ [Nm/rad])

Further, the CTC strategy is applied to control the XY-table with a stiffness of $k = 2.55[\text{Nm/rad}]$. From figure 4.5 and 4.6, it is seen that the controller ($\omega_0=15[\text{rad/s}]$ and $\beta_0=5$) has to do great efforts at realizing moderate results.

A reason for these disappointing results may be the need for a high damping ratio β_0 because otherwise the end-effector coordinates run out of reasonable bounds or numerical problems occur. The highly damped error system makes that the position and velocity errors have considerable magnitudes for a considerable time. These errors in combination with the heavy control gains result in the chattering effect of the input commands.

Both the results of the CRCTC and CTC strategy are considered relatively accurate. However, more powerful actuators are required in order to realize better results.

4.3 Trajectory tracking

4.3.1 The control problem

The second research topic is the realization of a prescribed circle in the XY-plane: $x_d = A\sin(\omega t)$ and $y_d = A\cos(\omega t)$ where $A=.1[\text{m}]$. The simulations are done for the circle ($T=2[\text{s}]$) that is applied in Lammerts [7]. As the desired trajectory of the end-effector is periodical with period time $T = 2\pi/\omega$, we want to compute a bounded, periodic solution $\rho_d(t)$. This problem is also translated to a two point boundary value problem in COLNEW with the boundary conditions $\rho_d(0) = \rho_d(t_e)$ and $\dot{\rho}_d(0) = \dot{\rho}_d(t_e)$. It is noted that the friction term which is mathematically described by $w_3 \text{atan}(1000\dot{x}_{3d})$ has to be removed from Eq.(2.7) because the algorithm does not converge when this term is included.

All the simulations for the trajectory tracking problem are done for the most flexible system. It is concluded on behalf of the results of the CRCTC strategy for the set-point tracking control problem that if the most flexible system shows good results this also will apply to the systems with less flexibility. First of all, it is tried to realize trajectory tracking if no initial position and velocity errors occur: $\underline{e} = \underline{0}$ and $\dot{\underline{e}} = \underline{0}$.

If this is possible, the next step is the realisation of the desired trajectory in spite of initial errors. These control problems are called respectively problem 1 and 2 in table 4.1. The CTC controlled system is called problem 3. Further, this table contains the used control gains.

4.3.2 Discussion of the results

The simulations without initial errors yield the results that are depicted in figure 4.7 and 4.8.

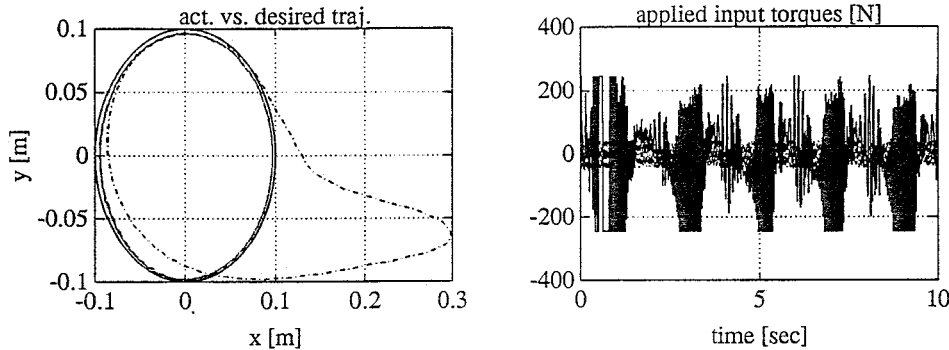


Figure 4.7: The described trajectory of the end-effector and the applied input torques u_1 (-) and u_2 (.) for the CRCTC strategy ($\dot{e} = e = 0$)

The desired end-effector trajectory is tracked reasonably well in the end. The X-coordinate shows a peak during the first transient. This phenomenon can be explained with the incorporation of the flexibility in the CRCTC strategy: the controller makes use of an elastic mode of the spindle in order to realize the desired trajectory. The elastic deformation of the spindle shows a vibration with the natural frequency of the spindle $f_0=7[Hz]$. This deformation is equal to a torsion of the spindle of approximately 1 [rad] with peaks of 6 [rad]. ($\varphi_3 - \varphi_1 = \frac{1}{r}(x_3 - x_1)$). The controller has to apply every 2 seconds a control command that 'chatters' for a few moments as the vibrations of the elastic deformation have to keep going by supplying energy to the system. From these input commands, it can be concluded that the controller has to do great efforts in order to realize the desired trajectory.

The big tracking error e_{rx_3} is remarkable because it is expected to become zero on base of the theory. It is tried to reduce this error by enlarging the third element of Λ . It is seen that this is difficult when K_r do not exist in Eq. (2.7). At the same time, the computed x_{3d} is an approximation which yields in some cases a non-reasonable, desired elastic deformation of approximately .2[m]. Therefore, it is concluded that this error should not be counted heavily.

Problem	Control gains	$e_x(t_e)$ [mm]	$e_y(t_e)$ [mm]
1	$K_r=[30 \ 10 \ 0]$ $\Lambda=[5 \ 5 \ 5]$ $K_i=[.8 \ .1 \ 0]$	5	4
2	$K_r=[30 \ 10 \ 0]$ $\Lambda=[6 \ 4 \ 6]$ $K_i=[.3 \ .2 \ 0]$	6	6
3	$\omega_0=30$ $\beta_0=1$	1	.5

Table 4.1: A survey of the results of the various controllers.

The CRCTC strategy is studied next when the end-effector starts in $O(0,0)$ without initial velocity. The results can be found in the figures 4.8 and 4.9 and are comparable with the above mentioned problem although the weight factors of e_x and e_{x_3} have to be enlarged. This fact is comprehensible as the controller has to be more exerted to realize the trajectory tracking in X-direction than in Y-direction because of the flexible spindle. An acceptable accuracy, see table 4.1, is combined with fast tracking in both cases. It is noted again that the obtained accuracy is limited by the used actuators. If better performances are desired, more powerfull actuators are required.

The results of the CTC strategy are shown in figure C.1 and C.2 and are compared with the CRCTC strategy. The CTC controller combines higher precision with strongly vibrating actuator commands. The elastic deformation is smaller but this is expected as x_{3d} is equal to x_d . This controller tracks x_{3d} reasonably well.

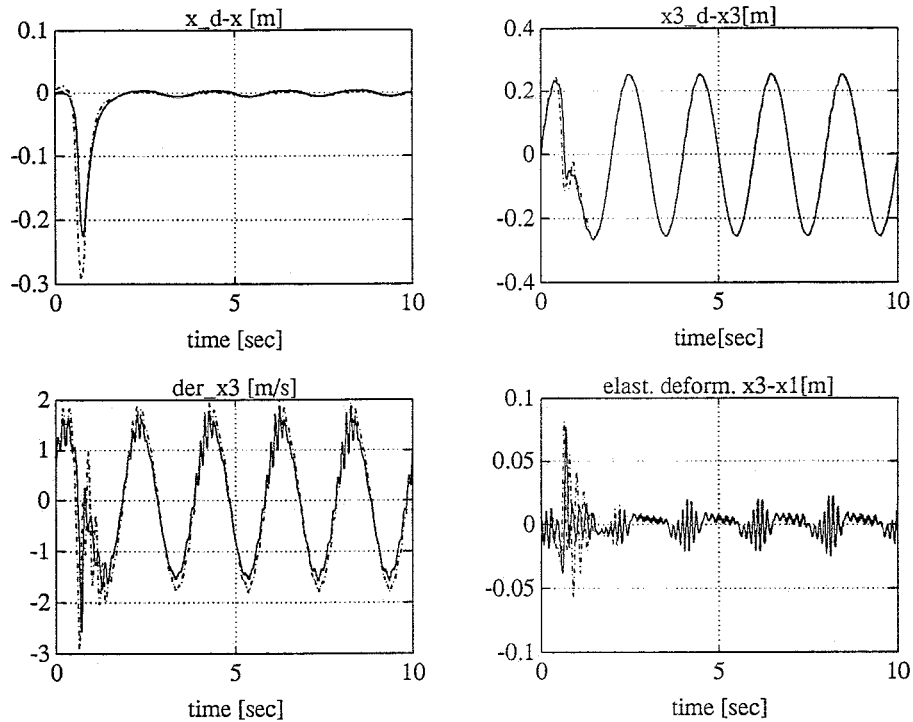


Figure 4.8: The results of the CRCTC strategy for: (1) the system without initial errors (-) and (2) when the end-effector starts in $O(0,0)$ (-.)

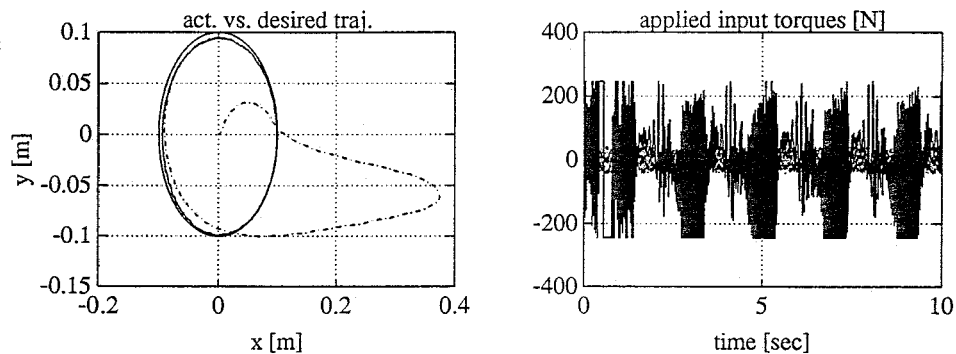


Figure 4.9: The described trajectory of the end-effector and the applied input torques for the CRCTC strategy. The end-effector starts in $O(0,0)$

Simulations are also done for the CTC strategy with use of the desired trajectory x_{3d} that is computed for the CRCTC strategy. The CTC strategy shows the same big error e_{x_3} . It can be demonstrated with these results that the controlled system is not been able to track at the same time the desired X-position of the end-effector and the desired trajectory of the flexible coordinate. The desired trajectories also lead to non-reasonable desired elastic deformation. Even

for very high control gains ($\omega_0 = 1000[\text{rad/s}]$ and $\beta_0 = 10$), the control objective can not anything like as approximated.

Finally, it is noted that all model parameters are supposed to be known exactly and no unmodeled dynamics exist during all the simulations. Therefore, this simulation environment is an ideal show case. In practice, the tracking performance is expected to decrease substantially.

Chapter 5

Conclusions and recommendations

5.1 Conclusions

- The simulations of the direct CRCTC strategy show promising results for both the set-point tracking and the trajectory tracking problem in spite of various approximations. It is emphasized that the results are obtained in an ideal simulation environment. For the most flexible system, $k = .46[Nm/rad]$, the desired trajectory is tracked quickly with a maximal position error in X and Y-direction of $6[mm]$. It is seen that the results improve when a modified version of the CTC strategy for flexible manipulators is used. However, the controlled system has to do great efforts in realizing these results for all the simulations. If better results are desired, more powerful actuators are required. In practice, the results are expected to decrease substantially.
- The implementation of the direct CRCTC strategy on the XY-table is realized. This implementation is time-consuming because the FORTRAN-package COLNEW and various programming languages have to be used.
- The available simulator and TCE-modules serve well with all the programming work. However, future experiments have to prove the value of the simulator. It is noted that the simulator runs some times into numerical problems. This can probably be brought on the modelled friction.

5.2 Recommendations

- The promising results justify further research. Future research should be concerned with the performance of the implemented strategy in practice. As the performance is expected to decrease for experiments, the direct CRCTC strategy can be expanded with an adaptation mechanism in order to cope with parametric uncertainty.
- Some attention has to be paid to the determination of the flexible coordinate. The value of the computed trajectory of the flexible coordinate should be examined because it can not always be realized by the controlled system. In other words, the necessity of the off-line determination should be inquired because the CTC strategy shows good results with the approximated, desired trajectory x_{3d} .

Bibliography

- [1] **Ascher, U.M., Christiansen, J. and Russell, R.D.** *COLSYS - a collocation code for boundary value problems.*, Lecture notes Comp.Sc. 76, Springer Verlag, B. Childs et al. (eds.), p.164-185, 1979.
- [2] **Banens, J.** *Documentation on TCE modules*, WFW-report 94.050.
- [3] **Banens, J.** *TCE simulator tools*, WFW-report 94.139.
- [4] **Brevoord, G.** *Composite Computed Torque Control of the XY table with an elastic motor transmission*, WFW-report 92.054
- [5] **Heeren, T.A.G.** *On control of manipulators*, Ph.D. thesis, Eindhoven University of Technology, Department of Mechanical Engineering, 1989.
- [6] **Koster, M.P.** *Dynamisch gedrag van constructies en mechanismen*, Lecture notes University of Technology Twente no. 113137 (in Dutch).
- [7] **Lammerts, I.M.M.** *Adaptive Computed Reference Computed Torque Control of flexible manipulators*, Ph.D. thesis, University of Technology Eindhoven, Department of Mechanical Engineering, 1993.

Appendix A

The model of the XY-table

A.1 The flexible model of the XY-table

The dynamic model of the flexible XY-table can be written as:

$$M(\underline{\varphi})\ddot{\underline{\varphi}} + C(\underline{\varphi}, \dot{\underline{\varphi}})\dot{\underline{\varphi}} + K\underline{\varphi} + \underline{w} \text{sign}(\dot{\underline{\varphi}}) = H\underline{u}$$

where $\underline{\varphi} = [\varphi_1 \ \varphi_2 \ \varphi_3]^T$ is the column of the generalized coordinates. The model matrices have the following structure:

$$M = \begin{bmatrix} M_{11} & 0 & M_{13} \\ 0 & M_{22} & M_{23} \\ M_{31} & M_{32} & M_{33} \end{bmatrix} \quad C = \begin{bmatrix} C_{11} & C_{12} & C_{13} \\ C_{21} & 0 & C_{23} \\ C_{31} & C_{32} & C_{33} \end{bmatrix}$$

$$K = \begin{bmatrix} K_{tot} & 0 & -K_{tot} \\ 0 & 0 & 0 \\ -K_{tot} & 0 & K_{tot} \end{bmatrix} \quad H = \begin{bmatrix} 1 & 0 \\ 0 & 1 \\ 0 & 0 \end{bmatrix} \quad \underline{w} = \begin{bmatrix} w_1 \\ w_2 \\ w_3 \end{bmatrix} \quad \underline{u} = \begin{bmatrix} u_1 \\ u_2 \end{bmatrix}$$

where:

$$\begin{aligned} M_{11} &= J_1 + (m_s + \frac{1}{3}m_t(\frac{l}{d})^2 + m_e(\frac{\varphi_2 r}{d})^2)r^2 \\ M_{13} &= M_{31} = (\frac{1}{2}m_t(\frac{l}{d}) - \frac{1}{3}m_t(\frac{l}{d})^2 + m_e(\frac{\varphi_2 r}{d}) - m_e(\frac{\varphi_2 r}{d})^2)r^2 \\ M_{22} &= J_2 + m_e r^2 \\ M_{23} &= M_{32} = m_e(\frac{(\varphi_1 - \varphi_3)r}{d})r^2 \\ M_{33} &= (m_s + m_t - m_t(\frac{l}{d}) + \frac{1}{3}m_t(\frac{l}{d})^2 + m_e - 2m_e(\frac{\varphi_2 r}{d}) + m_e(\frac{\varphi_2 r}{d})^2)r^2 \\ C_{11} &= m_e \varphi_2 r (\frac{r^3}{d^2}) \dot{\varphi}_2 \\ C_{12} &= C_{23} = m_e \varphi_2 r (\frac{r^3}{d^2}) (\dot{\varphi}_1 - \dot{\varphi}_3) \\ C_{13} &= -C_{11} \\ C_{21} &= -C_{12} \\ C_{31} &= m_e (d - \varphi_2 r) (\frac{r^3}{d^2}) \dot{\varphi}_2 \\ C_{32} &= m_e (d - \varphi_2 r) (\frac{r^3}{d^2}) (\dot{\varphi}_1 - \dot{\varphi}_3) \\ C_{33} &= -C_{31} \end{aligned}$$

The parameters in the model matrices are estimated in former research and have the following values:

$m_s=2.3[kg]$	$m_t=8.5[kg]$	$m_e=2.3[kg]$
$l=1.25[m]$	$d=1[m]$	$r=.01[m]$
$J_1=.0022[kgm^2]$	$J_2=.000158[kgm^2]$	$K_{tot}=k[Nm/rad]$
$w_1=30[Nm]$	$w_2=9[Nm]$	$w_3=20[Nm]$

A.2 The coordinate transformation

In order to design a direct control scheme, the dynamic model has to be transformed into a model with the generalized coordinates $\underline{y} = [x \ y \ x_3]^T$. Therefore, the following kinematic relationship is applied: $\underline{\varphi} = \Phi \underline{y}$.

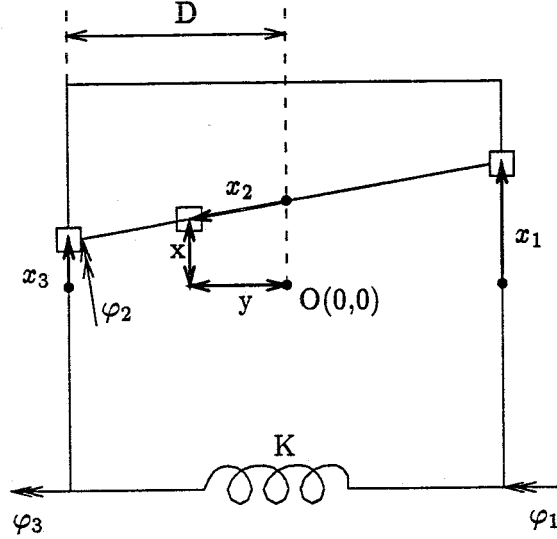


Figure A.1: The several coordinate systems

The following relationships can be extracted from figure A.1:

$$\begin{aligned}\varphi_1 &= \frac{1}{r}(x_3 + \frac{2D}{D-y}(x - x_3)) \\ \varphi_2 &= \frac{y}{r} \\ \varphi_3 &= \frac{x_3}{r}\end{aligned}$$

The first and second derivative of $\underline{\varphi}$ can be written as:

$$\underline{\dot{\varphi}} = \underline{\Psi} \underline{\dot{y}} \quad \text{where} \quad \Psi_{ij} = \frac{\delta \Phi_i}{\delta y_j}$$

and

$$\underline{\ddot{\varphi}} = \underline{\dot{\Psi}} \underline{\dot{y}} + \underline{\Psi} \underline{\ddot{y}} \quad \text{where} \quad \dot{\Psi} = \frac{\delta \Psi}{\delta y} \underline{\dot{y}}$$

The matrices $\underline{\Psi}$ and $\underline{\dot{\Psi}}$ are given by:

$$\underline{\Psi} = \frac{1}{r} \begin{bmatrix} \frac{2D}{D-y} & \frac{2D}{(D-y)^2}(x - x_3) & \frac{-(D+y)}{D-y} \\ 0 & 1 & 0 \\ 0 & 0 & 1 \end{bmatrix} \quad \underline{\dot{\Psi}} = \frac{2D}{r(D-y)^2} \begin{bmatrix} \dot{y} & \dot{x} - \dot{x}_3 + 2\dot{y} \frac{x-x_3}{D-y} & -\dot{y} \\ 0 & 0 & 0 \\ 0 & 0 & 0 \end{bmatrix}$$

Appendix B

Results of the set-point tracking problem

B.1 The model parameters

The dynamic model of the XY-table that is implemented in the simulator describes the flexible system with the generalized coordinates x_1 , x_2 and x_3 . For the meaning of this quantities, see figure A.1. As the model that is proposed in this study is formulated in the generalized coordinates x , y and x_3 , the model parameters have to be transformed to the new desired quantities of the simulator inputfile SIM.P.DAT.

$c = \frac{1}{r^2} k = 10^4 k [N/m]$
$m_0 = \frac{1}{r^2 i^2} J_1 = 1.03 [kg]$
$m_1 = \frac{1}{r^2} J_2 = 1.58 [kg]$

where i stands for the gear of the transmission. The input commands of Eq.(2.6) have to be divided by r^2 because the simulator requires input commands in $[N]$.

B.2 The results of simulations

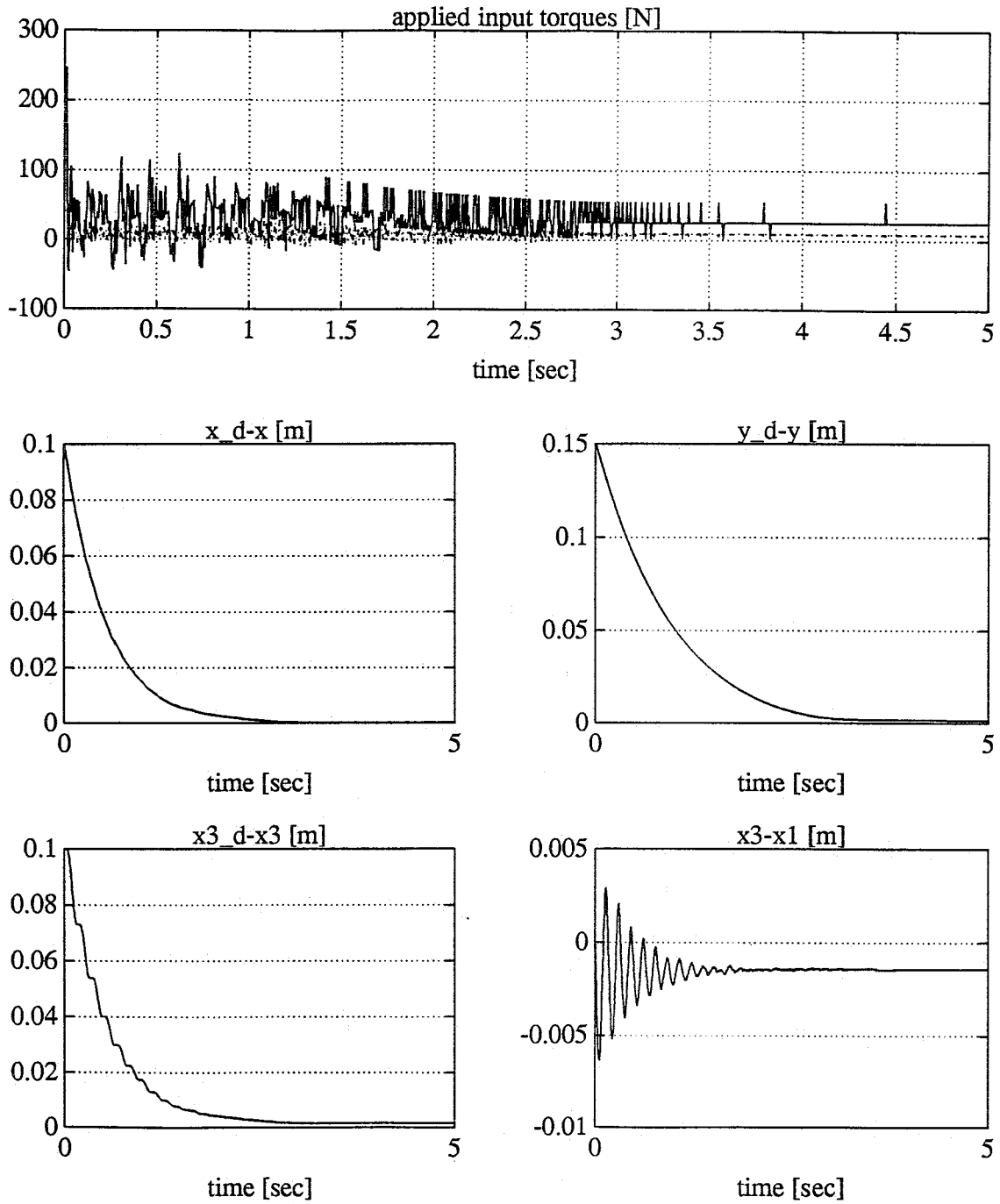


Figure B.1: *CRCTC* with $k = .46[\text{Nm/rad}]$ and $K_r = [30 \ 10]$, $\Lambda = [2 \ 1 \ 2]$ and $K_i = [.5 \ .3]$.

Appendix C

Results of the trajectory tracking problem

C.1 The results of the simulations

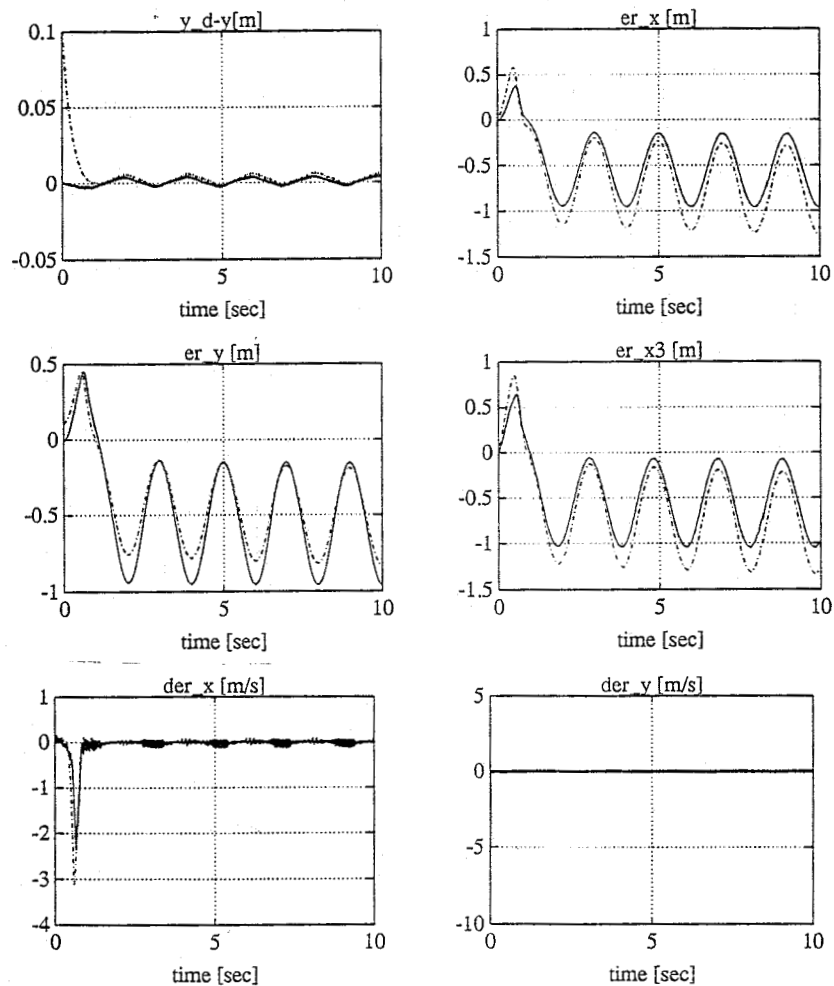


Figure C.1: CTC with $\omega_0 = 30[\text{rad/s}]$, $\beta_0 = 1$. The end - effector starts in $O(0,0)$.

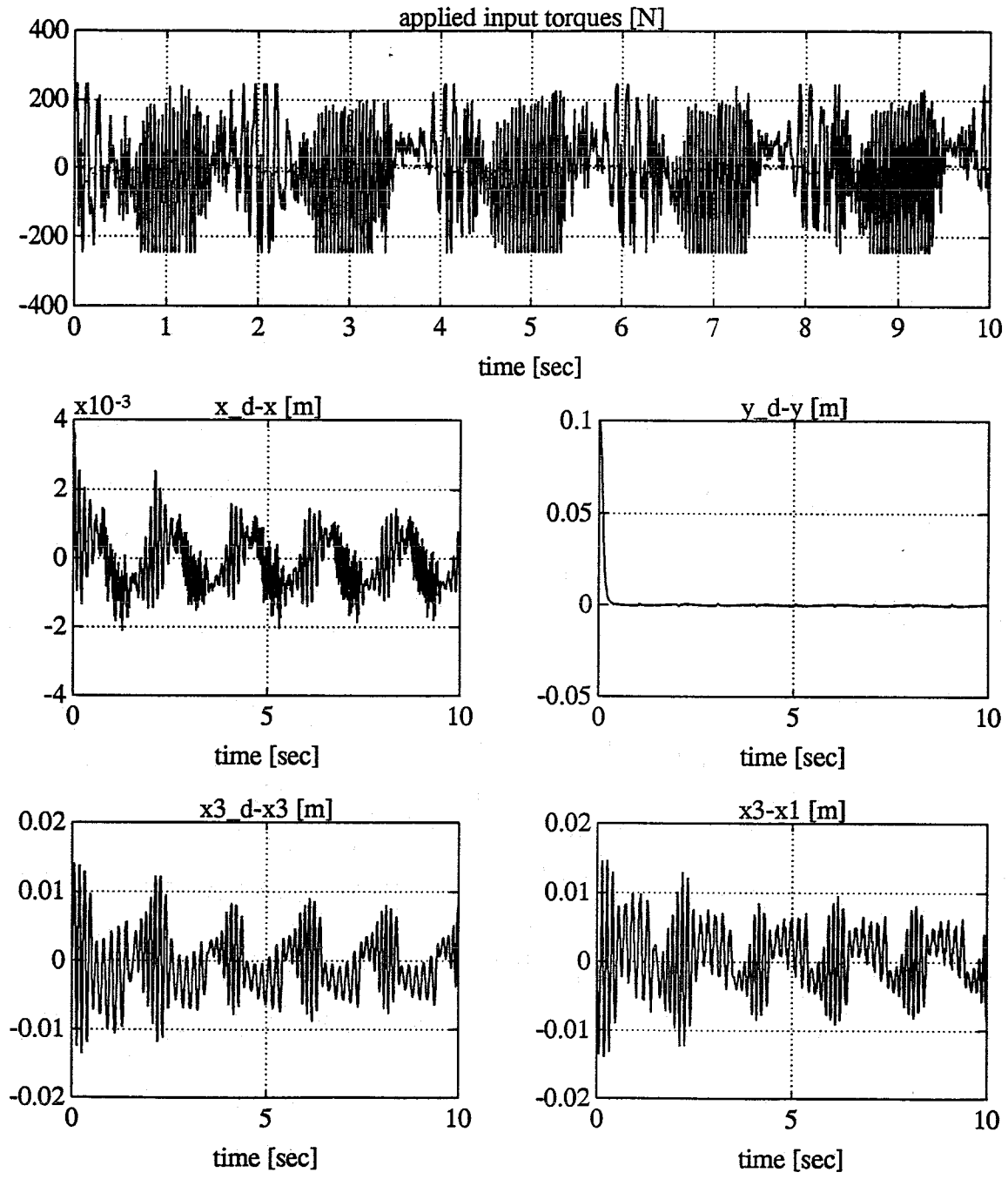


Figure C.2: CTC with $\omega_0 = 30[\text{rad/s}]$, $\beta_0 = 1$. The end - effector starts in $O(0,0)$.

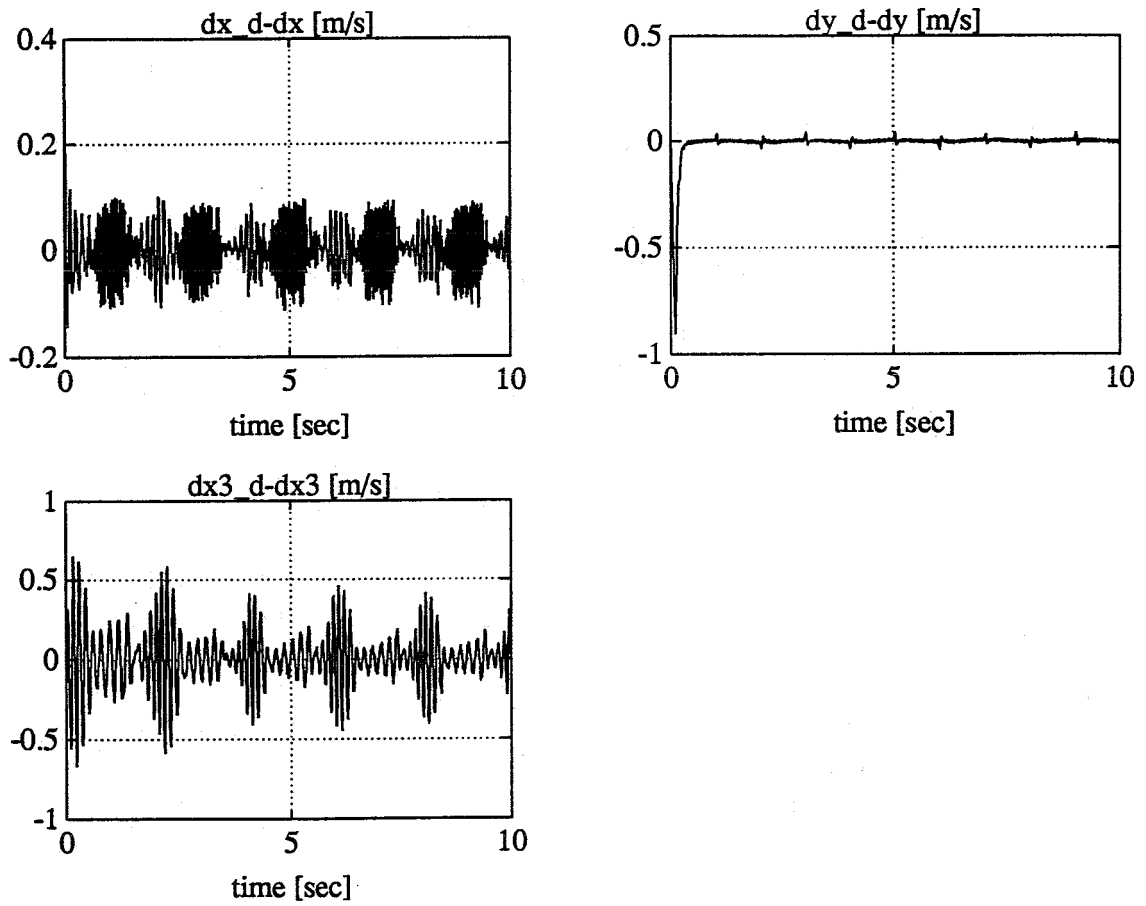


Figure C.3: CTC with $\omega_0 = 30[\text{rad/s}]$, $\beta_0 = 1$. The end-effector starts in $O(0, 0)$.